A multi-physics optimization problem in natural convection for a vertical channel asymmetrically heated

Delphine Ramalingom, Pierre-Henri Cocquet, Rezah Maleck, Alain Bastide

A multi-physics optimization problem in natural convection for a vertical channel asymmetrically heated

Delphine Ramalingom[a,*], Pierre-Henri Cocquet[a,*], Rezah Maleck[a], Alain Bastide[a]

[a] *Université de La Réunion, Laboratoire PIMENT, 117 Avenue du Général Ailleret, 97430 Le Tampon, France*

Abstract

This paper deals with a multi-physics topology optimization problem in an asymmetrically heated channel, considering both pressure drop minimization and heat transfer maximization. The problem is modeled under the assumptions of steady-state laminar flow dominated by natural convection forces. The incompressible Navier-Stokes equations coupled to the convection-diffusion equation through the Boussinesq approximation are employed and are solved with the finite volume method. In this paper, we first propose two new objective functions: the first one takes into account work of pressures forces and contributes to the loss of mechanical power while the second one is related to thermal power and is linked to the maximization of heat exchanges. In order to obtain a well-defined fluid-solid interface during the optimization process, we use a sigmoid interpolation function for both the design variable field and the thermal diffusivity. We also use adjoint sensitivity analysis to compute the gradient of the cost functional. Results are obtained for various Richardson (Ri) and Reynolds (Re) number such

*Corresponding author: delphine.ramalingom@univ-reunion.fr

Preprint submitted to International Journal of Heat and Mass Transfer October 20, 2017

that $100 < \mathrm{Ri} < 400$ and $\mathrm{Re} \in \{200, 400\}$. In all considered cases, our algorithm succeeds to enhance one of the phenomenon modelled by our new cost functions without deteriorating the other one. We also compare the values of standard cost functions from the litterature over iteration of our optimization algorithm and show that our new cost functions have no oscillatory behavior. As an additional effect to the resolution of the multi-physics optimization problem, we finally show that the reversal flow is suppressed at the exit of the channel.

Keywords: Natural convection, Mixed convection, Thermal power, Mechanical power, Sigmoid function, Vertical channel

1. Introduction

Topology optimization is a powerful and a popular tool for designers and engineers to design process. Its notion was initially introduced in structural mechanics by Bendsøe et al. [1]. In order to increase the structural stiffness under certain load, they targeted the optimal material density distribution by identifying areas in which material should be added. They expressed the design problem in terms of real valued continuous function per point, with values ranging from zero (indicating the presence of void/absence of material) to unity (indicating solid). The method has then been developed to numerous problems in structural mechanics [2, 3, 4, 5, 6, 7, 8]. In fluid mechanics, the same idea was adapted to Stokes flows by Borrvall and Petersson [9], by introducing a real-valued inverse permeability multiplied by a kinematic viscosity dependent term into the flow equations. Domain areas corresponding to the fluid flow are those where α is equal to 0 or, in practice,

inferior or equal to a user-defined positive number α_0. Domain areas where α value are not equal to 0 or superior to α_0 define the part of the domain to be solidified [10]. The optimal solid walls to be designed correspond to the interfaces between the two aforementioned areas. So, the goal of topology optimization is to compute the optimal α field in order to minimize some objective function under consideration.

Contrary to topology optimization applied to design structure, research on topology optimization applied to heat transfer and fluid dynamics is quite recent. Dbouk [11] presented a review about topology optimization design methods that have been developed for heat transfer systems, and for each of them, he presented their advantages, limitations and perspectives. In topology optimization problems with large number of design variables, gradient-based algorithms are frequently used to compute accurate solutions efficiently [12, 13, 14, 15, 16, 17]. This algorithm starts with a given geometry and iterates with information related to the derivatives (sensitivity derivatives) of the objective function with respect to the design variables. Among the methods used to compute the sensitivity derivatives required by gradient-based methods, the adjoint method [12, 18, 19, 20, 13] has been receiving a lot of attention since the cost of computing the necessary derivatives is independent from the number of design variables. Papoutsis-Kiachagias and Giannakoglou [19] present a review on continuous adjoint method applied to topology optimization for turbulent flows. Othmer [20] derived the continuous adjoint formulations and the boundary conditions on ducted flows for typical cost functions. He proposed an objective function that conduct to reduce pressure drop in open cavity. The originality of his method is the

versatility of the formulation where the adjoint boundary conditions were expressed in a form that can be adapted to any commonly used objective function. Then, for the automotive industry, Othmer et al. [21] implemented several objective functions like dissipated power, equal mass flow through different outlets and flow uniformity. To describe the transition and interface between two different materials in the domain, the Solid Isotropic Material with Penalization (SIMP) technique [1, 22] is the mostly used in the literature as the interpolation technique in topology optimization. This approach represents the non-fluid regions as infinitely stiff, a penalty to the flow, such that no interaction is modeled. Yoon [17] presented a method for solving static fluid-structure interaction problems by converting the stresses at the fluid/solid interfaces into a volume integral representation. A new method of interpolation in order to improve the interface fluid/solid during the optimization process was presented by Ramalingom et al. [10]. They proposed to use two sigmoid functions in order to interpolate material distribution and thermal conductivity and show that the transition zones, that is the zones where the velocity of the fluid is too large to be considered as solid, can be made arbitrary small.

Convection typically is categorized, according to fluid motion origins, as forced, mixed or natural [23, 24]. All aforementioned references on heat transfer problems are dealt in case of forced or mixed convection. This means that the fluid motion is driven by a fan, pump or pressure gradient often modeled by a non-null velocity at entrance of the studied domain. Natural convection involves a heat dissipation mechanism where the fluid motion is governed by differences in buoyancy arising from temperature gradients. More precisely,

the fluid is submitted to a small velocity, the corresponding heat rates are also much lower than those associated with forced convection. Bruns [16] applied topology optimization to convection-dominated heat transfer problems. He highlighted numerical instabilities in convection-dominated diffusion problems and justified them by the density-design-variable-based topology optimization. Alexandersen et al. [25] applied topology optimization to natural convection problems. He obtained complex geometries that improved the cooling of heat sinks. They encountered difficulties as oscillatory behaviour of the solver, namely a damped Newton method, used for the optimization computations. They also reported intermediate relative densities that amplified the natural convection effects leading to non-vanishing velocity in some solid parts of the computational domain. As a result, those zones are considered as solid by the optimization algorithm while they should be treated as fluid. Both authors used filtering techniques in order to avoid numerical instabilities [26, 27, 28, 13, 14].

In this paper, we deal with some topology optimization problems for heat and mass transfers, considering the physical case of an asymmetrically heated vertical channel. This geometry has been subject to numerous studies in the literature [29, 30, 31, 32]. The first investigations date back to 1942 with the works of Martinelli and Boelter [33] according to the comprehensive review of Jackson et al. [34]. Developing and fully developed laminar free convection within heated vertical plates was subsequently investigated numerically by Bodoia and Osterle [35] and was experienced by Elenbaas [36]. Since then, many studies were carried out. This great interest can be explained by the fact that this configuration is encountered in several industrial devices

such as solar chimney, energy collectors, electronic components and even in nuclear reactors. The optimization of these systems simultaneously demands compactness, efficiency and control of heat and mass transfers.

This paper investigates numerical instabilities that can be developed in convection-dominated diffusion problems [37, 16]. Instead of proposing methods to improve filtering techniques and avoid these instabilities, we propose a new expression of objective functions within the framework of topology optimization applied to an asymmetrically heated vertical channel. The geometry considered here is the model proposed by Desrayaud et al. [38] and corresponding to a boundary layer flow with a reversal flow at the exit [39] . We study the influence of Richardson number, which represents the importance of natural convection relative to the forced convection, in the optimized design. Our optimization algorithm succeeds especially to suppress the reversal flow and to increase the thermal exchanges in the channel for the range of Richardson numbers considered. Moreover, no numerical instabilities have been encountered during the optimization process and no filter techniques have been used. We finally compare the stability of our results at the end of the optimization process to those obtained with classical cost functions of the literature.

2. Governing equations

The flows considered in this paper are assumed to be in a steady-state laminar regime, newtonian and incompressible. Figure 1 shows the configuration of the computational domain Ω.

Physical properties of the fluid are kinematic viscosity ν and thermal

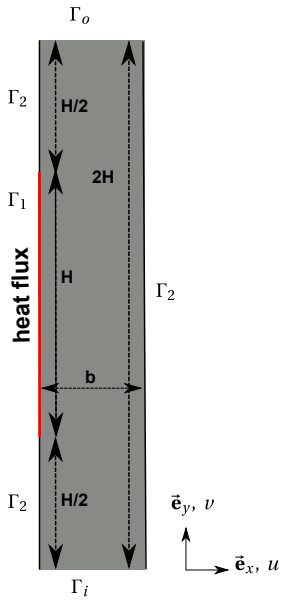

Figure 1: Geometry of the problem

conductivity λ_f. First, parameters governing the flow is the Reynolds number defined as $\mathrm{Re} = U\ b/\nu$, with b being the width of the channel and U the reference velocity based on the average velocity at the channel entrance. The Prandtl number is defined as $\mathrm{Pr} = \nu/k$. It describes the ratio between the momentum and thermal diffusivities of the fluid. For $\mathrm{Pr} < 1$, the energy is transferred to the fluid by heat conduction since it prevails over convection. For $\mathrm{Pr} > 1$ the energy is transferred through the fluid mainly thanks to convection. In this paper, we consider only fluids with small Prandtl that is $\mathrm{Pr} < 1$. The Grashof number is defined as $\mathrm{Gr}_b = g\ \beta\ \Delta T\ b^3/\nu^2$ and represents the ratio between buoyancy and viscous force. $\Delta T = -\phi/\lambda$, ϕ is the thermal flux on Γ_1 and λ is the thermal conductivity of the fluid. In thermal convection problems, Richardson number $\mathrm{Ri} = \mathrm{Gr}_b/\mathrm{Re}^2$ represents the importance of natural convection relative to the forced convection. For values

superior to unity, we know that the flow is dominated by natural convection. Under these assumptions and thanks to a method given in Borrvall and Petersson [9], the porosity field is introduced in the steady-state Navier-Stokes equation as a source term $h_\tau(\alpha)\mathbf{u}$ which yields a Brinkman-like model with a convection term. Therefore, the dimensionless form of the Navier-Stokes and energy equations are written as follows:

$$\begin{aligned} \nabla \cdot \mathbf{u} &= 0 && \text{in } \Omega \\ (\mathbf{u} \cdot \nabla)\ \mathbf{u} &= -\nabla p + \mathrm{Re}^{-1}\Delta \mathbf{u} - h_\tau(\alpha)\mathbf{u} + \mathrm{Ri}\ \theta\ \overrightarrow{e_y} && \text{in } \Omega \\ \nabla \cdot (\mathbf{u}\theta) &= \nabla \cdot (\mathrm{Re}^{-1}\mathrm{Pr}^{-1} k_\tau(\alpha)\nabla\theta) && \text{in } \Omega \end{aligned} \tag{1}$$

where $(\mathbf{u}, p, \theta)$ correspond respectively to dimensionless velocity, pression and temperature and are usually referred as the primal variable in the curent setting. Parameter α is the spatially varying design variable field determined by the optimization algorithm. For the natural-dominated convection problem, we consider the following boundary conditions:

$$\begin{aligned} &\mathbf{u} = 0, && \nabla p = 0, && \partial_n \theta = -1 && \text{on } \Gamma_1, \\ &\mathbf{u} = 0, && \nabla p = 0, && \partial_n \theta = 0 && \text{on } \Gamma_2, \\ &\mathbf{u} = u_i \mathbf{e}_y, && \nabla p = 0, && \theta = 0 && \text{on } \Gamma_i, \\ &\partial_n \mathbf{u} = 0, && p = 0, && \partial_n \theta = 0 && \text{on } \Gamma_o, \end{aligned} \tag{2}$$

where ∂_n is the normal derivative defined as $\partial_n = n \cdot \nabla$.

3. Topology optimization formulation

The main goal of this paper is to solve a multi-physics optimization problem in the asymmetrically heated channel, considering both pressure drop

minimization described by a first objective function $\mathcal{J}_1$ and heat transfer maximization described by a second objective function $\mathcal{J}_2$. The optimization problem can be stated as:

$$\begin{aligned} &\text{minimize:} && \mathcal{J} = \gamma_1\, \mathcal{J}_1 + \gamma_2\, \mathcal{J}_2, \\ &\text{subject to:} && \text{Governing equations (1),} \\ & && \text{Boundary conditions (2).} \end{aligned} \tag{3}$$

where the cost function $\mathcal{J}$ is the combination of the two objectives functions, γ_1 and γ_2 are weighting coefficients. It is easy to observe that, for $\gamma_1 \gg \gamma_2$, the multi-objective function is directed to a minimum power dissipation problem, while for $\gamma_1 \ll \gamma_2$, a maximum heat dissipation problem arises.

3.1. Cost functions

As indicated by several authors [28, 13, 18, 15], cost functions $\mathcal{J}_1$ and $\mathcal{J}_2$ are expressions of multi-physics powers that one either wish to minimize or to maximize. A classical cost function used by Marck et al. [13], Othmer [20] for evaluating total pressure losses is :

$$f(\mathbf{u}, p) = \int_\Gamma -\mathbf{n}\cdot\mathbf{u}\ \left(p + \frac{1}{2}\ |u|^2\right) \mathrm{d}S. \tag{4}$$

Also, Marck et al. [13], Kontoleontos et al. [18] evaluate the thermal power by this expression:

$$f(\mathbf{u}, \theta) = \int_\Gamma \mathbf{n}\cdot\mathbf{u}\ \theta\ \mathrm{d}S. \tag{5}$$

In our study, we propose to evaluate mechanical power and thermal power via two new expressions of both cost functions. As we will show below, these functions avoid numerical instabilities encountered in convection-dominated

diffusion optimization problems and do not require the use of filter techniques. They will also permit to stabilize the optimization process. For a system with an inlet, an outlet, an average velocity and an average temperature, we define the thermal power as the product of the mass flow, the volume heat capacity and the difference of temperature between the entrance and the exit of the system. Likewise, mechanical power is defined as the product of mass flow rate and the difference of total pressure between the entrance and the exit of the system. In that way, we chose the work of pressure forces to minimize the power dissipated in the channel as used in systemic approach. Hence, the first cost function can be written as:

$$\begin{aligned} \mathcal{J}_1(\mathbf{u},p) = \; & -\frac{1}{|\Gamma_i|}\int_{\Gamma_i} p_t \, \mathrm{d}S \int_{\Gamma_i} \mathbf{u}\cdot\mathbf{n} \, \mathrm{d}S \\ & -\frac{1}{|\Gamma_o|}\int_{\Gamma_o} p_t \, \mathrm{d}S \int_{\Gamma_o} \mathbf{u}\cdot\mathbf{n} \, \mathrm{d}S, \end{aligned} \tag{6}$$

where $p_t = p + 1/2 \; \mathbf{u}^2$ is the total pressure, Γ_i and Γ_o are respectively the entrance and the exit of the channel.

The second cost function concerns thermal exchange maximization and is given by:

$$\begin{aligned} \mathcal{J}_2(\mathbf{u},p) = \; & \frac{1}{|\Gamma_i|}\int_{\Gamma_i} \theta \, \mathrm{d}S \int_{\Gamma_i} \mathbf{u}\cdot\mathbf{n} \, \mathrm{d}S \\ & +\frac{1}{|\Gamma_o|}\int_{\Gamma_o} \theta \, \mathrm{d}S \int_{\Gamma_o} \mathbf{u}\cdot\mathbf{n} \, \mathrm{d}S. \end{aligned} \tag{7}$$

3.2. Multi-objective optimization

In multi-objective optimization, the challenge is to benefit from both objective functions. As introduced in previous subsection, the objective function based on maximization of thermal exchanges can involve the increase of pressure drop and conversely for the objective function relative to the dissipation of power. The set of solutions can be reached by using an Aggregate

Objective Function (AOF), also known as the weighted-sum approach, which is based on a linear combination of both objective functions [40, 41]. Before combining linearly the two functions, they must then be rescaled to have the same order of magnitude. This can be achieved as follows:

$$\hat{f} = \frac{f - f_{min}}{f_{max} - f_{min}} \tag{8}$$

where f is either $\mathcal{J}_1$ or $\mathcal{J}_2$. As explicated by Marck et al. [13], the other four parameters are determined by solving both optimization problems independently (3) for min $\mathcal{J}_1$ and max $\mathcal{J}_2$ with maximal porosity (α_{max}). Consequently, both rescaled objective functions are ranged between 0 and 1. Such a rescaling allows to consider the following linear combination:

$$\hat{\mathcal{J}} = \omega\ \hat{\mathcal{J}}_1 - (1 - \omega)\hat{\mathcal{J}}_2 \tag{9}$$

where ω is the weight balancing the influence of each objective function ($\omega \in [0, 1]$). Note that this combination involves the opposite of $\mathcal{J}_2$ since the optimization algorithm aims at minimizing the combinatory function $\hat{\mathcal{J}}$. Thereafter, $\hat{\mathcal{J}}_1$ and $\hat{\mathcal{J}}_2$ are used only during the optimization process.

4. Topology optimization methods

Applying topology optimization to this problem aims to minimize an objective function $\mathcal{J}$ by finding an optimal distribution of solid and fluid element in the computational domain. The goal of topology optimization is to end up with binary designs, i.e avoid that the design variables take other value than those representing the fluid or the solid. This is usually carried out by penalizing the intermediate densities with respect to the material parameters,

such as inverse permeability and effective conductivity. A standard approach is to use interpolation functions. We also use gradient-based algorithm that relies on the continuous adjoint method.

4.1. Interpolation functions

The additional term $h_\tau(\alpha)$ in (1) physically corresponds to the ratio of a kinematic viscosity and a permeability. The interpolation function for the thermal diffusivity of each element is $k_\tau(\alpha)$, both functions were defined in Ramalingom et al. [10]. Regions with very high permeability can be considered as solid regions, and those with low permeability regions are interpreted as pure fluid.

Inverse permeability is thus interpolated with the following formula

$$h_\tau(\alpha) = \alpha_{max} \left(\frac{1}{1 + \exp\left(-\tau(\alpha - \alpha_0)\right)} - \frac{1}{1 + \exp\left(\tau\alpha_0\right)} \right), \tag{10}$$

where α_0 is the abscissa slope of the sigmoid function, α_{max} is the maximum value that the design parameter α can take and is set to $2\ 10^5$. In Ramalingom et al. [10], it is shown that the parameter α_0 is linked to the quantity of material added in the domain Ω. In the present study, we chose $\alpha_0 = 20$.

The difference in the adimensional thermal conductivities of the fluid and solid regions in considered through the interpolation of effective conductivity k_τ as follows:

$$k_\tau(\alpha) = \frac{1}{k_f} \left[k_f + (k_s - k_f) \left(\frac{1}{1 + \exp\left(-\tau(\alpha - \alpha_0)\right)} - \frac{1}{1 + \exp\left(\tau\alpha_0\right)} \right) \right], \tag{11}$$

where k_s and k_f are respectively the thermal diffusivity of the fluid domains and the thermal conductivity of solid domains.

4.2. Adjoint problem

The Lagrange multiplier method [42] is used to get an optimization problem without constraints and can be used to get the sensitivity of the cost function $\mathcal{J}$. The Lagrangian is defined as

$$\begin{aligned} &\mathcal{L}(\mathbf{u}, p, \theta, \mathbf{u}^*, p^*, \theta^*, \alpha) = \mathcal{J}(\mathbf{u}, p, \theta) \\ &+ \int_\Omega \mathcal{R}(\mathbf{u}, p, \theta) \cdot (\mathbf{u}^*, p^*, \theta^*) d\Omega, \end{aligned} \tag{12}$$

where $(\mathbf{u}^*, p^*, \theta^*)$ are the adjoint variables and $\mathcal{R}(\mathbf{u}, p, \theta) = 0$ corresponds to the governing equations (1). The critical points of $\mathcal{L}$ with respect to the adjoint variables give the constraint of the optimization problem (3) while the critical point with respect to the primal variable yield the so-called adjoint problem. The latter can be derived as in Othmer [20] (see also [10]) and is given by

$$\begin{aligned} \nabla p^* - h_\tau(\alpha)\mathbf{u}^* + \theta\ \nabla\theta^* + \ Re^{-1}\Delta\mathbf{u}^* + \nabla\mathbf{u}^*\ \mathbf{u} - (\mathbf{u}^*\cdot\nabla)\mathbf{u} \ &= 0 \quad \text{in} \quad \Omega, \\ \nabla\cdot\mathbf{u}^* \ &= 0 \quad \text{in} \quad \Omega, \\ Ri\ \mathbf{u}^*\cdot\overrightarrow{e_y} + \mathbf{u}\cdot\nabla\theta^* + \nabla\cdot(Re^{-1}Pr^{-1}k_\tau(\alpha)\nabla\theta^*) \ &= 0 \quad \text{in} \quad \Omega, \end{aligned} \tag{13}$$

together with the boundary conditions

$$\begin{aligned} &\mathbf{u}^* = 0,\ \partial_n\theta^* = 0,\ \partial_n p^* = 0 && \text{on } \Gamma_1 \cup \Gamma_2, \\ &u_t^* = 0,\ \theta^* = 0,\ \frac{\partial\mathcal{J}}{\partial p} = -u_n^*,\ \partial_n p^* = 0 && \text{on } \Gamma_i, \\ &u_t^* = 0,\ \frac{\partial\mathcal{J}}{\partial\theta} = -\theta^*\ u_n - Re^{-1}Pr^{-1}k_\tau(\alpha)\partial_n\theta^* && \text{on } \Gamma_o, \\ &\frac{\partial\mathcal{J}}{\partial\mathbf{u}}\cdot\mathbf{n} = -p^* - \theta^*\ \theta - Re^{-1}\ \partial_n\mathbf{u}^*\cdot\mathbf{n} - u_n^*\ u_n - \mathbf{u}\cdot\mathbf{u}^* && \text{on } \Gamma_o, \end{aligned} \tag{14}$$

where $u_n = \mathbf{u} \cdot \mathbf{n}$ and the derivatives of $\mathcal{J}$ defined in (3) with respect to $(\mathbf{u},\ p,\ \theta)$ are given by

$$\begin{aligned}
\left.\frac{\partial \mathcal{J}}{\partial p}\right|_{\Gamma_i} &= -\gamma_1\ \frac{1}{|\Gamma_i|}\int_{\Gamma_i} \mathbf{u}\cdot\mathbf{n}\ \mathrm{d}S \\
\left.\frac{\partial \mathcal{J}}{\partial \theta}\right|_{\Gamma_o} &= \ \ \gamma_2\ \frac{1}{|\Gamma_o|}\int_{\Gamma_o} \mathbf{u}\cdot\mathbf{n}\ \mathrm{d}S \\
\left.\frac{\partial \mathcal{J}}{\partial \mathbf{u}}\right|_{\Gamma_o} &= -\gamma_1\ \frac{1}{|\Gamma_o|}\mathbf{n}\int_{\Gamma_o} p_t\ \mathrm{d}S - \gamma_1\ \mathbf{u}\cdot\int_{\Gamma_o}\mathbf{u}\cdot\mathbf{n}\ \mathrm{d}S \\
&\quad +\ \gamma_2\ \frac{1}{|\Gamma_o|}\mathbf{n}\int_{\Gamma_o}\theta\ dS.
\end{aligned} \tag{15}$$

We emphasize that the adjoint problem (13,14) has been derived for the cost function $\mathcal{J}$ given by (3). Nevertheless, in the numerical result, we wish to minimize the rescaled cost function $\hat{\mathcal{J}}$ whose derivatives with respect to $(\mathbf{u},\ p,\ \theta)$ are obtained thanks to (15) with

$$\gamma_1 = \frac{\omega}{\mathcal{J}_{1,max} - \mathcal{J}_{1,min}},\ \gamma_2 = \frac{-(1-\omega)}{\mathcal{J}_{2,max} - \mathcal{J}_{2,min}}.$$

4.3. Implementation

Topology optimization problem is solved by iterative calculations. The main steps of the algorithm for the topology optimization consist to compute sensitivities by adjoint method and evaluate the optimality condition. If a stopping criterion is met, the computation is terminated. The forward problem (1) and the adjoint problem (13) are implemented using OpenFOAM [43]. The optimality condition is given by the critical point of the Lagrangian with respect to the design parameter α as follows:

$$\begin{aligned}
&\frac{\partial h_\tau}{\partial \alpha}\ \mathbf{u}\cdot\mathbf{u}^* + \frac{\partial k_\tau}{\partial \alpha}\nabla\theta\cdot\nabla\theta^* = 0 \quad \text{in } \Omega, \\
&\frac{\partial k_\tau}{\partial \alpha}\ \theta^* = 0 \ \text{ with } \partial_n\theta = -1 \qquad \text{on } \Gamma_1.
\end{aligned} \tag{16}$$

The design variables are evaluated by using the conjugated-gradient descent direction method associated to Polack-Ribiere method. To summarize, the algorithm for the topology optimization is described in Table 1.

Step 0.	Initialization: set all the constants Re, Ri, Pr
Step 1.	Solve the forward problem (1),(2) problem with the Finite Volume Method
Step 2.	Compute objective and constraint values
Step 3.	Compute sensitivities by adjoint method
Step 4.	Evaluate the optimality condition. If a stopping criterion is met, terminate the calculation.
Step 5.	Project design variable α with $\alpha_k = \max(0, \min(\alpha, \alpha_{\max}))$
Step 6.	Update design variables α with $\alpha_{k+1} = -\nabla \mathcal{J}_{k+1} + \beta_{k+1}^{PR}\ \alpha_k$ and return to step 1

Table 1: Algorithm of topology optimization

5. Results

First of all, it is important to note that the problem is purely academic and the values of various parameters as Prandtl number set to 0.71 corresponding to a fluid/liquid, and k_s/k_f have been therefore set to three. As they are in the range of realistic problems, they are thought to be representative of the problems that can be physically encountered.

The problem is investigated for $\mathrm{Ri} = \{100, 200, 400\}$ under constant $\mathrm{Re} = 400$ which is equivalent to increase the dominance of natural convection in the conducto-convection problem. These values have been chosen in accordance with the study of Li et al. [44] on reversal flows in the asymmetrically heated channel. The problem is also investigated for $\mathrm{Re} = 200$ and $\mathrm{Ri} = 400$ in order to highlight the effect of convection on the optimization results. We

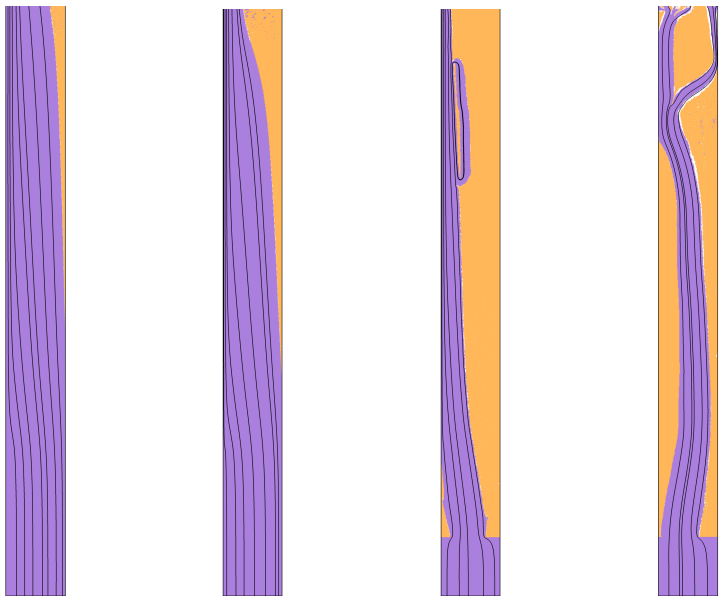

(a) Ri = 100, $Q_t = 4.9\%$ (b) Ri = 200, $Q_t = 13.3\%$ (c) Ri = 400, $Q_t = 52.2\%$ (d) Obtained with (4) and (5) Ri = 100, $\omega = 0.5$

Figure 2: Optimized designs and streamtraces at various Ri for constant Re = 400. Orange corresponds to solid material and purple corresponds to the fluid domain.

chose $\alpha_0 = 20$ and set α_{max} to $2 \cdot 10^5$ keeping in mind that similar results have been obtained for $\alpha_{max} = 10^6$.

Figure 3a shows the vertical velocity profile at the entrance of the channel for the two values of Re. For this study, we chose different values of ω in accordance with the importance given to the different costs function $\mathcal{J}_1$ or $\mathcal{J}_2$. All results performed in this paper correspond to physical quantities, that is $\mathcal{J}_1$ and $\mathcal{J}_2$. Moreover, in order to be sure that no material is added at the entrance of the channel during the optimization process, we solved

the problem by imposing fluid domain at the lower part of the channel, i.e. $\alpha = 0$ for the element in $[0,1] \times [0,1]$.

5.1. Varying Ri *at constant* Re $= 400$

It can be seen that the obtained designs at varying Ri (Figure 2) differ from one another, which is to be expected.

First of all, when the natural convection forces become more dominant, the optimization algorithm adds more material in the channel. We compute the proportion Q_t of material added in the domain Ω as follows:

$$Q_t = \frac{\int_\Omega h_\tau(\alpha)\ d\Omega}{\alpha_{max}\ V_{tot}},\ \text{where } V_{tot} \text{ is the total volume of } \Omega. \tag{17}$$

The proportion of material added in the vertical channel varies from 4.9% to 52.2%. It is referenced on Figure 2. Hence, the quantity of material increases when Richardson number increases.

Secondly, we can observe that the structure of the flow in the channel is modified. From Figure 2c, it can be seen that for Ri $= 400$, all of the material is kept close to the right wall of the domain and the flow circulation is obliged to be near the heated wall. This contributes to the second objective function corresponding to increase the thermal exchanges in the channel. Besides, temperature profiles at the exit of the channel are shown on Figure 3b.

It can also be observed that the flow reversal is suppressed after optimization process. Indeed, material added by the algorithm at the end of the channel prevent the fluid from re-entering in the channel. As can be seen on Figure 4, vertical component of the velocity has a positive value in the channel after optimization and is null or very small in the solid region, as expected. That means our interpolation function gives an optimized design

with no physical error as a non-null velocity in the solid regions without connectivity (Kreissl and Maute [45] and Lee [28]). Moreover, value of vertical component of the velocity increases when Ri increases (cf. Figure 3b). That is due to the reduction of the section for the flow circulation which causes an acceleration of the fluid in the channel. The width of flow circulation after optimization is referenced on Figure 5. It demonstrates also that the sigmoid function $h_\tau(\alpha)$ which interpolates the design variable α affects correctly volume elements to solid domains in order to avoid checkerboards. That brings to a well definition of the frontier fluid-solid as obtained by Ramalingom et al. [10].

With regard to cost functions computation at the end of the optimization process, we highlight the influence of Ri on thermal power and mechanical power. Indeed, as the Richardson number increases, the power due to work forces decreases and the thermal power in the channel increases. Figure 6 gives the computation of cost functions before optimization process and after the optimization. Hence, $\mathcal{J}_1$ is reduced by a factor 1.64 and $\mathcal{J}_2$ is reduced by a factor 1.51 (Table 2) for $\mathrm{Re} = 400$ and for $\mathrm{Ri} = 100$. When we compare $\mathcal{J}_1$ to its value without optimization $\mathcal{J}_1\mathrm{Ref}$, we notice that sometimes the optimization algorithm added material which contributes to rising friction forces and pressure losses as long as the heat dissipation increases. Hence, for the case $(\mathrm{Re}, \mathrm{Ri}) = (400, 200)$, $\mathcal{J}_1$ is reduced by a factor 1.13 while $\mathcal{J}_2$ is increased by a factor 0.46. On the contrary, for the case $(\mathrm{Re}, \mathrm{Ri}) = (400, 400)$, $\mathcal{J}_1$ is increased by a factor 0.26 while $\mathcal{J}_2$ is reduced by a factor 0.64. These cases illustrated that our algorithm permits to add material in the channel in order to contribute to one or other cost functions according to the weighted

coefficient ω. Hence, for the case $(\mathrm{Re}, \mathrm{Ri}) = (400, 200)$, we chose to prioritize the minimization of mechanical power with $\omega = 0.85$. For the case $(\mathrm{Re}, \mathrm{Ri}) = (400, 400)$, we chose to prioritize the maximization of heat transfer with $\omega = 0.15$. We can conclude that the algorithm succeeds to minimize/maximize one or other cost functions by adding material without penalizing too much to one or other.

Figure 7 shows the computation of thermal power and mechanical power at each iteration of the optimization process. We can compare the evolution throughout iterations for the classical cost functions of the literature (Figure 7a) and for the cost functions proposed in our study (Figure 7a). Contrary to the cost functions (6) and (7), classical cost functions (4) and (5) present an oscillatory behavior when applied to our dominated-natural-convection problem. These instabilities lead to important oscillations of the adjoint pression and the adjoint velocity (cf. Equation (13)). Moreover, as mathematical sign of velocity switches, our algorithm adds material in the domain in accordance with the optimality condition (cf. Equation (3)). Therefore, these numerical instabilities lead to a optimized design with a lot of quantity of material (Figure 2d) evaluated at $Q_t = 45.03\%$. Hence, we can conclude that the new expression of both cost functions gives a better stability of the computation at the end of the optimization process.

5.2. Constant $\mathrm{Ri} = 400$ *and* $\mathrm{Re} = 200$

In Li et al. [44], the authors considered the case $\mathrm{Re} = 200$ and $\mathrm{Ri} = 400$, which gives a dimensionless length of the reversal flows the most important of their study. As for $\mathrm{Re} = 400$, we observe that the reversal flow is suppressed (cf. Figure 8b). A lot of material is added in the channel computed at

(Re, Ri)	(400, 100)	(400, 200)	(400, 400)	(200, 400)
$\mathcal{J}_1$ref/$\mathcal{J}_1$	1.64	1.13	0.26	3.60
$\mathcal{J}_2$ref/$\mathcal{J}_2$	1.51	0.46	0.64	3.09

Table 2: Reduction factor of cost functions - ref corresponds to the value of cost functions without optimization

$Q_t = 53.5\%$. The section for the circulation flow is also reduced. It is evaluated at $d = 0.16$, being the smallest width of circulation flow in this study. The flow circulation is thus imposed near the heated wall (cf. Figure 8a). Temperature field Figure 8b shows that heat surface exchanges are increased thanks to the material added by the algorithm. This phenomenon contributes to the objective function $\mathcal{J}_2$. Table 2 indicates that $\mathcal{J}_1$ is reduced by a factor 3.6 and $\mathcal{J}_2$ is increased by a factor 3.09, knowing $\omega = 0.5$ for this simulation case. It is important to note that for Re = 200, we can observe a very low vertical component of the velocity of 10^{-5} in some parts of the solid material (cf. 8b). So, when the vertical component of the velocity is higher, more material is added such as the section for the circulation flow is smaller. Velocity at the exit is higher and the thermal/mechanical power is respectively increased/reduced by a factor approximately 3.

6. Conclusion

A multi-physics optimization problem considering both pressure drop minimization and heat transfer maximization in the asymmetrically heated channel has been examined. The problem is handled in natural convection with several values of Richardson number. First of all, two objective func-

tions are investigated representing the work of forces for the mechanical power and heat exchanges with the thermal power. In accordance with the physical problem considered, a weighted coefficient is chosen for the combined cost function. These functions allow to obtain optimal designs and they are relatively reduced in accordance with the weight affected to each of them. Several conclusions have been drawn. First of all, the reversal flow in the channel is suppressed at the end of the optimization. That contributes to reducing the loss of charges in the channel. Then, the new cost functions contribute to avoid the use of filter techniques as no numerical instabilities are observed. The stability of the computation at the end of the optimization process is better than this obtained with classical cost functions of the literature. For $\mathrm{Re} = 400$, vertical component of the velocity increases when Ri number increases. The section for the circulation of flow is reduced. Concerning the fluid-solid boundary, they are well-definited during the optimization process thanks to two sigmoid functions used for the interpolation of both the design variable and the thermal diffusivity. Finally, the optimization algorithm is able to increase thermal exchanges while maintaining the loss of charges due to friction, thanks to the combined objective functions used. In conclusion, this study highlights the importance of the expression of cost function in a topology optimization problem. The influence of the Richardson is observed on vertical velocity value and on the quantity of material added in the optimized channel. As future work, we suggest a more complete heat and mass transfer model might be considered, as pure natural convection problems and radiation problems.

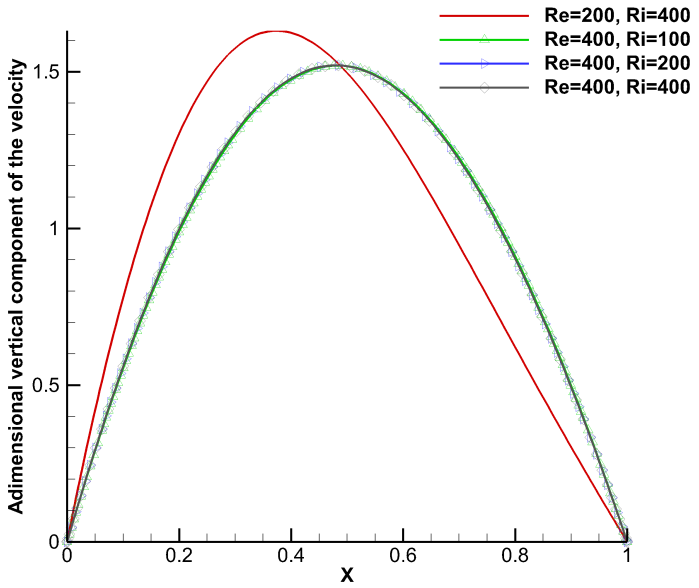

(a)

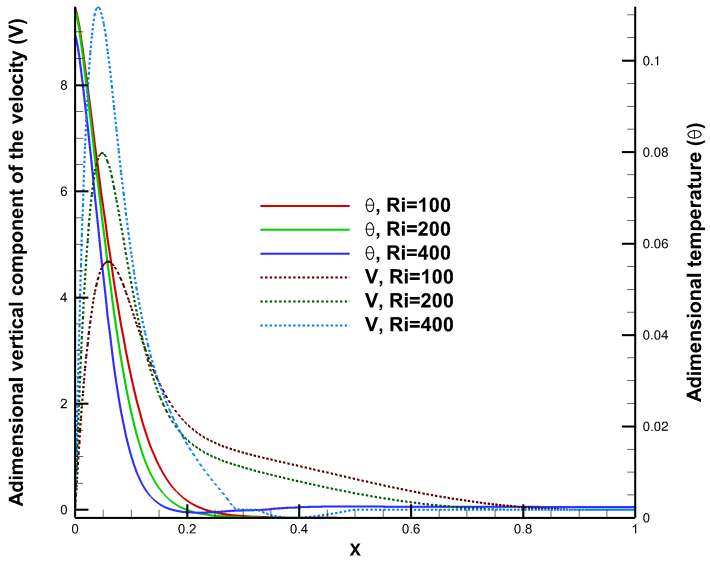

(b)

Figure 3: Adimensional vertical component of the velocity for Re = $\{200, 400\}$ (a), Temperature and vertical component of the velocity (b) at the end of the hot plate of the channel $y = 3H/2$

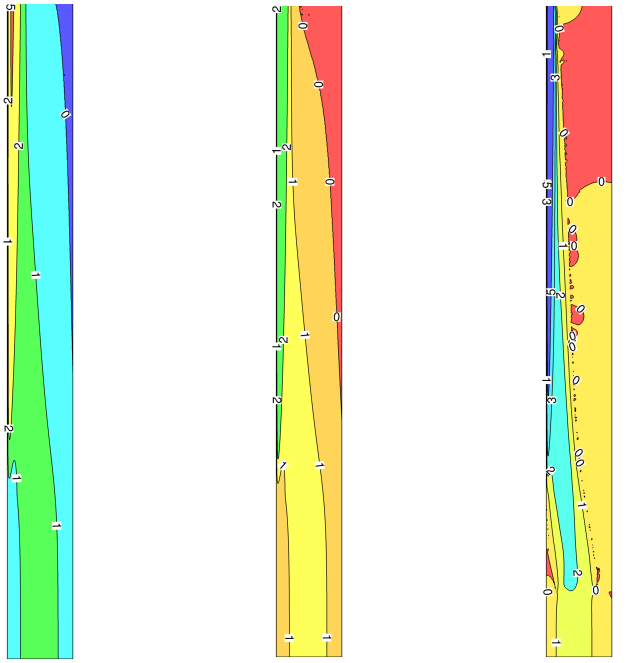

(a) Ri = 100 $\omega = 0.5$ (b) Ri = 200 $\omega = 0.85$ (c) Ri = 400 $\omega = 0.15$

Figure 4: Adimensional vertical velocity at various Ri for constant Re = 400

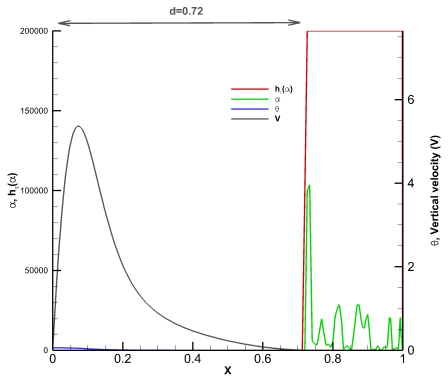

(a) Re = 400, Ri = 100

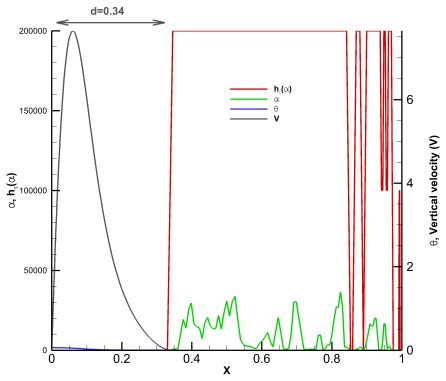

(b) Re = 400, Ri = 200

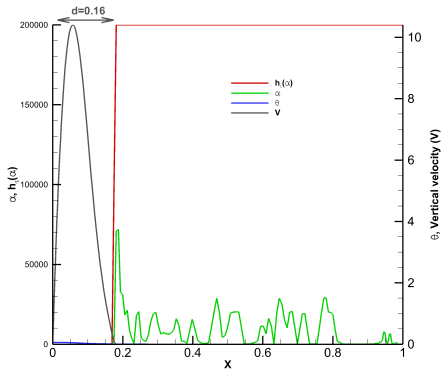

(c) Re = 400, Ri = 400

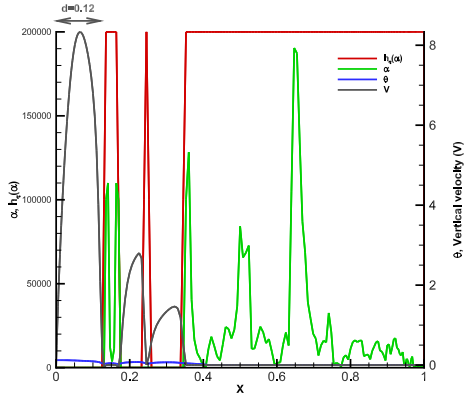

(d) Re = 200, Ri = 400

Figure 5: Adimensional temperature, vertical velocity, α and h(α) at the end section of the channel and for various Ri for constant Re = 400 - annotation d is used for the width of the flow section

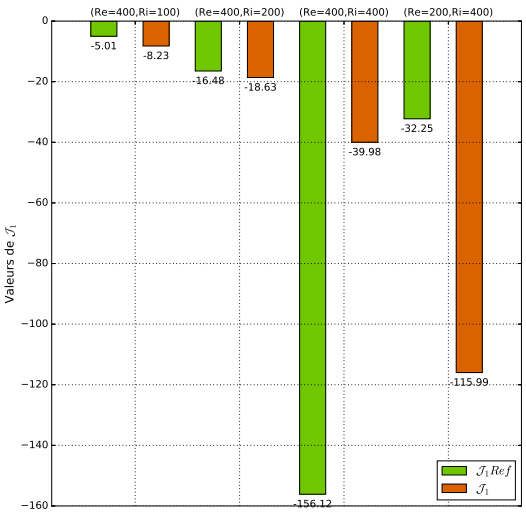

(a) $\mathcal{J}_1$ values

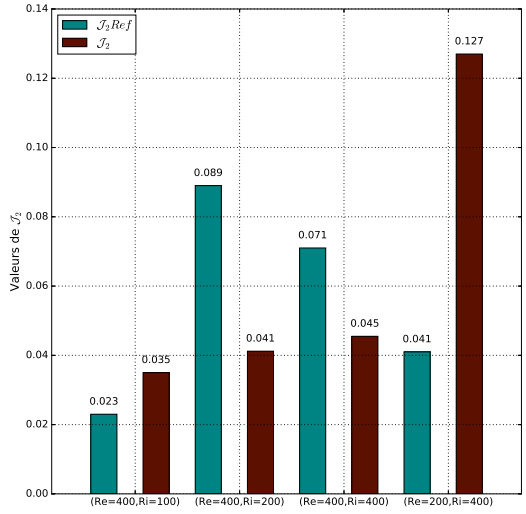

(b) $\mathcal{J}_2$ values

Figure 6: Mechanical power (a) and thermal power (b) without optimization noticed Ref and after optimization

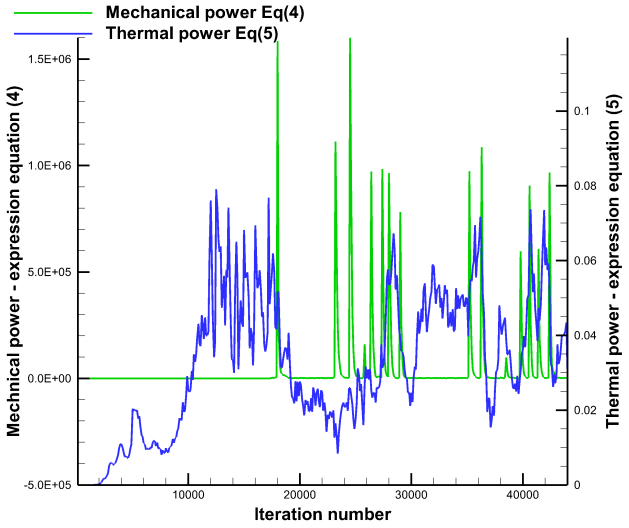

(a) Values of classical cost functions (4) and (5) over iterations for the minimization of $\hat{\mathcal{J}}$

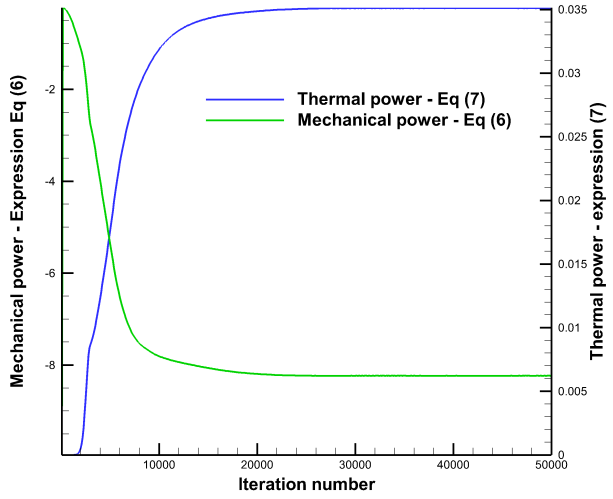

(b) Values of new cost functions (6) and (7)over iterations for the minimization of $\hat{\mathcal{J}}$

Figure 7: Comparison of cost functions computations throughout iterations - Re $=$ 400, Ri $= 100$, $\omega = 0.5$

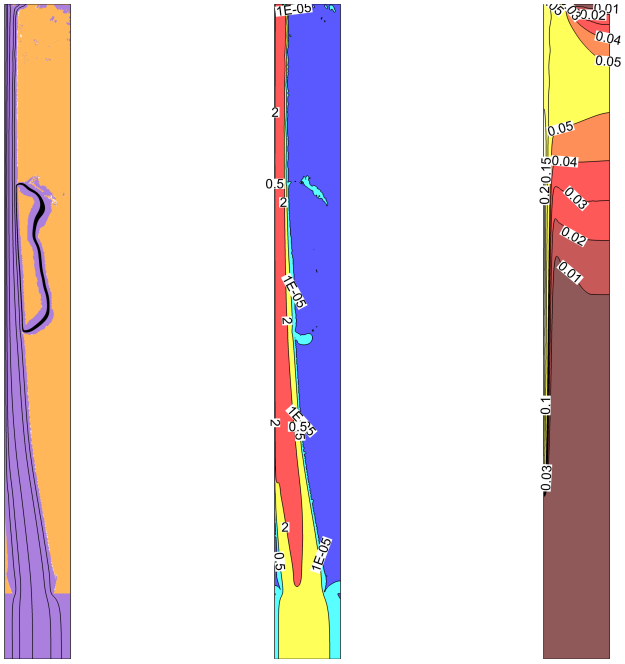

(a) (b) (c)

Figure 8: Optimization results for constant Re = 200 and Ri = 400: Optimized design, $\omega = 0.5$ (a), Adimensional vertical component of the velocity (b), Adimensional temperature field (c)

References

[1] M. P. Bendsøe, N. Kikuchi, M. P. Bendsoe, N. Kikuchi, M. P. Bendsøe, N. Kikuchi, Generating optimal topologies in structural design using a homogenization method, Computer Methods in Applied Mechanics and Engineering 71 (2) (1988) 197–224, ISSN 00457825, doi:\bibinfo{doi}{10.1016/0045-7825(88)90086-2}, URL http://linkinghub.elsevier.com/retrieve/pii/0045782588900862.

[2] O. Sigmund, K. Maute, Topology optimization approaches: A comparative review, doi:\bibinfo{doi}{10.1007/s00158-013-0978-6}, 2013.

[3] H. A. Eschenauer, N. Olhoff, Topology Optimization of Continuum Structures: A review*, Applied Mechanics Reviews 54 (4) (2001) 331–390, ISSN 00036900, doi:\bibinfo{doi}{10.1115/1.1388075}, URL http://appliedmechanicsreviews.asmedigitalcollection.asme.org/article.aspx?articleid=1396619.

[4] O. Q. Liang, Performance-based optimization: A review, Advances in Structural Engineering 10 (6) (2007) 739–753, ISSN 1369-4332, doi:\bibinfo{doi}{10.1260/136943307783571418}, URL <GotoISI>://WOS:000252480600012.

[5] B. Hassani, E. Hinton, A review of homogenization and topology opimization IIanalytical and numerical solution of homogenization equations, Computers & Structures 69 (6) (1998) 719–738, ISSN 00457949, doi:\bibinfo{doi}{10.1016/S0045-7949(98)00132-1}.

[6] B. Hassani, E. Hinton, A review of homogenization and topology optimization Ihomogenization theory for media with periodic structure, Computers & Structures 69 (6) (1998) 707–717, ISSN 00457949, doi:\bibinfo{doi}{10.1016/S0045-7949(98)00131-X}.

[7] B. Hassani, E. Hinton, Review of homogenization and topology optimization III - topology optimization using optimality criteria, Computers and Structures 69 (6) (1998) 739–756, ISSN 00457949, doi:\bibinfo{doi}{10.1016/S0045-7949(98)00133-3}.

[8] M. Y. Wang, X. Wang, D. Guo, A level set method for structural topology optimization, Computer Methods in Applied Mechanics and Engineering 192 (1-2) (2003) 227–246, ISSN 00457825, doi:\bibinfo{doi}{10.1016/S0045-7825(02)00559-5}.

[9] T. Borrvall, J. Petersson, Topology optimization of fluids in Stokes flow, International Journal for Numerical Methods in Fluids 41 (1) (2003) 77–107, ISSN 02712091, doi:\bibinfo{doi}{10.1002/fld.426}, URL `http://doi.wiley.com/10.1002/fld.426`.

[10] D. Ramalingom, P.-H. Cocquet, A. Bastide, A new interpolation technique to deal with fluid-porous media interfaces for topology optimization of heat transfer, Submitted .

[11] T. Dbouk, A review about the engineering design of optimal heat transfer systems using topology optimization, Applied Thermal Engineering 112 (2016) 841–854, ISSN 13594311, doi:\bibinfo{doi}{10.1016/

435 j.applthermaleng.2016.10.134}, URL http://linkinghub.elsevier.
436 com/retrieve/pii/S135943111632645X.

437 [12] C. Othmer, Adjoint methods for car aerodynamics, Journal of Math-
438 ematics in Industry 4 (1) (2014) 6, ISSN 2190-5983, doi:\bibinfo{doi}
439 {10.1186/2190-5983-4-6}, URL http://www.mathematicsinindustry.
440 com/content/4/1/6.

441 [13] G. Marck, M. Nemer, J.-L. Harion, Topology optimization of
442 heat and mass transfer problems: laminar flow, Numerical Heat
443 Transfer, Part B: ... 63 (6) (2013) 508–539, ISSN 1040-7790,
444 doi:\bibinfo{doi}{10.1080/10407790.2013.772001}, URL http://www.
445 tandfonline.com/doi/abs/10.1080/10407790.2013.772001.

446 [14] J. Alexandersen, N. Aage, C. S. Andreasen, O. Sigmund, Topol-
447 ogy optimisation for natural convection problems, International Jour-
448 nal for Numerical Methods in Fluids 76 (10) (2014) 699–721,
449 ISSN 02712091, doi:\bibinfo{doi}{10.1002/fld.3954}, URL http://
450 doi.wiley.com/10.1002/fld.3954.

451 [15] A. A. Koga, E. C. C. Lopes, H. F. Villa Nova, C. R. D. Lima,
452 E. C. N. Silva, Development of heat sink device by using topol-
453 ogy optimization, International Journal of Heat and Mass Trans-
454 fer 64 (2013) 759–772, ISSN 00179310, doi:\bibinfo{doi}{10.1016/j.
455 ijheatmasstransfer.2013.05.007}, URL http://dx.doi.org/10.1016/
456 j.ijheatmasstransfer.2013.05.007.

457 [16] T. E. Bruns, Topology optimization of convection-dominated, steady-

state heat transfer problems, International Journal of Heat and Mass Transfer 50 (15-16) (2007) 2859–2873, ISSN 00179310, doi:\bibinfo{doi}{10.1016/j.ijheatmasstransfer.2007.01.039}.

[17] G. H. Yoon, Topological design of heat dissipating structure with forced convective heat transfer, Journal of Mechanical Science and Technology 24 (6) (2010) 1225–1233, ISSN 1738494X, doi:\bibinfo{doi}{10.1007/s12206-010-0328-1}.

[18] E. a. Kontoleontos, E. M. Papoutsis-Kiachagias, a. S. Zymaris, D. I. Papadimitriou, K. C. Giannakoglou, Adjoint-based constrained topology optimization for viscous flows, including heat transfer, Engineering Optimization 0273 (December) (2012) 1–21, ISSN 0305-215X, doi:\bibinfo{doi}{10.1080/0305215X.2012.717074}.

[19] E. M. Papoutsis-Kiachagias, K. C. Giannakoglou, Continuous Adjoint Methods for Turbulent Flows, Applied to Shape and Topology Optimization: Industrial Applications, Archives of Computational Methods in Engineering 23 (2) (2016) 255–299, ISSN 18861784, doi:\bibinfo{doi}{10.1007/s11831-014-9141-9}, URL http://link.springer.com/10.1007/s11831-014-9141-9.

[20] C. Othmer, A continuous adjoint formulation for the computation of topological and surface sensitivities of ducted flows, International Journal for Numerical Methods in Fluids 58 (8) (2008) 861–877, ISSN 02712091, doi:\bibinfo{doi}{10.1002/fld.1770}, URL http://doi.wiley.com/10.1002/fld.1770.

[21] C. Othmer, T. Kaminski, R. Giering, Computation of Topological Sensitivities in Fluid Dynamics : Cost Function Versatility, Eccomas Cfd (2006) 1–12.

[22] M. Zhou, G. I. N. Rozvany, The COC algorithm, Part II: Topological, geometrical and generalized shape optimization, Computer Methods in Applied Mechanics and Engineering 89 (1-3) (1991) 309–336, ISSN 00457825, doi:\bibinfo{doi}{10.1016/0045-7825(91)90046-9}.

[23] F. White, Fluid Mechanics, McGraw-Hill,New York (2010) 862ISSN 1364-0321, doi:\bibinfo{doi}{10.1111/j.1549-8719.2009.00016.x.Mechanobiology}, URL http://www.amazon.com/Mechanics-Student-McGraw-Hill-Mechanical-Engineering/dp/0077422414.

[24] F. P. Incropera, D. P. Dewitt, Introduction To Heat Transfer, Igarss 2014 (1) (2014) 1–5, ISSN 13514180, doi:\bibinfo{doi}{10.1007/s13398-014-0173-7.2}.

[25] J. Alexandersen, O. Sigmund, N. Aage, Large scale three-dimensional topology optimisation of heat sinks cooled by natural convection, International Journal of Heat and Mass Transfer 100 (2016) 876–891, ISSN 00179310, doi:\bibinfo{doi}{10.1016/j.ijheatmasstransfer.2016.05.013}, URL http://dx.doi.org/10.1016/j.ijheatmasstransfer.2016.05.013.

[26] B. S. Lazarov, O. Sigmund, Filters in topology optimization based on Helmholtz-type differential equations, International Journal for Numer-

ical Methods in Engineering 86 (6) (2011) 765–781, ISSN 00295981, doi:\bibinfo{doi}{10.1002/nme.3072}.

[27] T. E. Bruns, A reevaluation of the SIMP method with filtering and an alternative formulation for solid-void topology optimization, Structural and Multidisciplinary Optimization 30 (6) (2005) 428–436, ISSN 1615147X, doi:\bibinfo{doi}{10.1007/s00158-005-0537-x}.

[28] K. Lee, Topology Optimization of Convective Cooling System Designs, Ph.D. thesis, University of Michigan, 2012.

[29] E. Bacharoudis, M. G. Vrachopoulos, M. K. Koukou, D. Margaris, A. E. Filios, S. A. Mavrommatis, Study of the natural convection phenomena inside a wall solar chimney with one wall adiabatic and one wall under a heat flux, Applied Thermal Engineering 27 (13) (2007) 2266–2275, ISSN 13594311, doi:\bibinfo{doi}{10.1016/j.applthermaleng.2007.01.021}.

[30] F. P. Incropera, Convection Heat Transfer in Electronic Equipment Cooling, Journal of Heat Transfer 110 (4b) (1988) 1097, ISSN 00221481, doi:\bibinfo{doi}{10.1115/1.3250613}.

[31] R. B. Yedder, E. Bilgen, Natural convection and conduction in Trombe wall systems, International Journal of Heat and Mass Transfer 34 (4-5) (1991) 1237–1248, ISSN 00179310, doi:\bibinfo{doi}{10.1016/0017-9310(91)90032-A}.

[32] B. F. Balunov, A. S. Babykin, R. A. Rybin, V. A. Krylov, V. N. Tanchuk, S. A. Grigoriev, Heat transfer at mixed convection in vertical and inclined flat channels of the vacuum chamber of the ITER international

thermonuclear reactor, High Temperature 42 (1) (2004) 126–133, ISSN 0018151X, doi:\bibinfo{doi}{10.1023/B:HITE.0000020100.11937.3f}.

[33] R. C. Martinelli, L. M. K. Boelter, The Analytical Prediction of Superposed Free and Forced Viscous Convection in a Vertical Pipe, by RC Martinelli and LMK Boelter..., University of California Press, 1942.

[34] J. D. Jackson, M. A. Cotton, B. P. Axcell, Studies of mixed convection in vertical tubes, International journal of heat and fluid flow 10 (1) (1989) 2–15.

[35] J. R. Bodoia, J. F. Osterle, The Development of Free Convection Between Heated Vertical Plates, Journal of Heat Transfer 84 (1) (1962) 40–43, ISSN 0022-1481, URL http://dx.doi.org/10.1115/1.3684288.

[36] W. Elenbaas, Heat dissipation of parallel plates by free convection, Physica 9 (1) (1942) 1–28, ISSN 00318914, doi:\bibinfo{doi}{10.1016/S0031-8914(42)90053-3}, URL http://www.sciencedirect.com/science/article/pii/S0031891442900533.

[37] G. H. Yoon, Y. Y. Kim, The element connectivity parameterization formulation for the topology design optimization of multiphysics systems, International Journal for Numerical Methods in Engineering 64 (12) (2005) 1649–1677, ISSN 00295981, doi:\bibinfo{doi}{10.1002/nme.1422}.

[38] G. Desrayaud, E. Chénier, A. Joulin, A. Bastide, B. Brangeon, J. P. Caltagirone, Y. Cherif, R. Eymard, C. Garnier, S. Giroux-Julien, Others, Y. Harnane, P. Joubert, N. Laaroussi, S. Lassue, P. Le Quéré,

R. Li, D. Saury, A. Sergent, S. Xin, A. Zoubir, Benchmark solutions for natural convection flows in vertical channels submitted to different open boundary conditions, International Journal of Thermal Sciences 72 (January 2009) (2013) 18–33, ISSN 12900729, doi:\bibinfo{doi}{10.1016/j.ijthermalsci.2013.05.003}, URL http://linkinghub.elsevier.com/retrieve/pii/S1290072913001130.

[39] D. Ramalingom, P.-h. Cocquet, A. Bastide, Numerical study of natural convection in asymmetrically heated channel considering thermal stratification and surface radiation, Numerical Heat Transfer, Part A: Applications .

[40] T. W. Athan, P. Y. Papalambros, A Note on Weighted Criteria Methods for Compromise Solutions in Multi-Objective Optimization, doi:\bibinfo{doi}{10.1080/03052159608941404}, 1996.

[41] A. Messac, C. Puemi-Sukam, E. Melachrinoudis, Aggregate objective functions and pareto frontiers: Required relationships and practical implications, Optimization and Engineering 1 (2) (2000) 171–188, ISSN 1389-4420.

[42] H. Everett III, Generalized Lagrange multiplier method for solving problems of optimum allocation of resources, Operations research 11 (3) (1963) 399–417, ISSN 0030-364X.

[43] G. H. W. Et al., A tensorial approach to computational continuum mechanics using object- oriented techniques, Computers in physics 12.6 (1998) 620–631.

[44] R. Li, M. Bousetta, E. Chénier, G. Lauriat, Effect of surface radiation on natural convective flows and onset of flow reversal in asymmetrically heated vertical channels, International journal of thermal sciences (2013) 9–27URL http://ac.els-cdn.com/S1290072912002979/1-s2.0-S1290072912002979-main.pdf?{_}tid=8a08949c-5533-11e4-a420-00000aab0f6b{\&}acdnat=1413464237{_}a1a20230e1ac1cf44957235fdc24b3cf.

[45] S. Kreissl, K. Maute, Levelset based fluid topology optimization using the extended finite element method, Structural and Multidisciplinary Optimization 46 (3) (2012) 311–326, ISSN 1615147X, doi:\bibinfo{doi}{10.1007/s00158-012-0782-8}.